Astronomical and Astrophysical Transactions (*AApTr*), 2024, Vol. 34, Issue 3, pp. 277–294,
ISSN 1055-6796, Photocopying permitted by license only, ©Cambridge Scientific Publishers

Exoplanets on close-in orbits around their host stars (HD 209458 b)

E.S. Belenkaya[1,*], A.S. Krotov[1,2], I.I. Alexeev[1], A.S. Lavrukhin[1]

[1] *Skobeltsyn Institute of Nuclear Physics, FSBIHE Lomonosov Moscow State University, 1(2) Leninskie Gory, 119991, Moscow, Russian Federation*
[2] *Faculty of Physics, FSBIHE Lomonosov Moscow State University, 1(2) Leninskie Gory, 19991, Moscow, Russian Federation*

Received 7 July, 2024; accepted 17 September, 2024

The conditions in the stellar wind at the close orbit of the exoplanet HD 209458 b, previously also known as Osiris in honor of the Egyptian god, are examined in detail. It is shown that depending on the conditions in the stellar wind flowing around the planet, the structure of its magnetosphere changes dramatically. Studying the stellar wind is made easier by the fact that the central star HD 209458 is a solar-type yellow dwarf. In 2014, magnetic field of HD 209458 b was indirectly estimated by studying the escape of hydrogen from the exoplanet's environment. Using a paraboloid model of the magnetosphere developed for exoplanets, the structure of the magnetosphere was constructed depending on the Alfvén Mach number, M_A, and stellar wind's magnetic field. It is shown how, with an increase in the magnitude of the magnetic field of the stellar wind and, accordingly, with a decrease in the Alfvén Mach number to values less than 1, Alfvén wings arise instead of a comet-like magnetosphere with a bow shock in front of it. Alfvén wings create a direct connection between the exoplanet and the host star, carried out by a magnetic field.

Keywords: Exoplanets; stars; magnetic field; Alfvén Mach number; Alfvén wings

1 Introduction

Since the 1990s, the study of exoplanets – planets outside the Solar system – has been actively developing. The study of these objects is carried out both through observations using constantly improving instruments and technology and by constructing theories of their formation and evolution. The properties of different types of exoplanets and the relationships between their characteristics are studied. There are currently (May 2024) 5632 confirmed exoplanets[1].

*Email: elena.belenkaya.msu@gmail.com

[1] `NASA Exoplanet Archive (https://exoplanetarchive.ipac.caltech.edu/)`

To date, there are no confirmed direct measurements of the magnetic field of exoplanets, although the search for radio emission, which would allow it to be calculated, is actively underway. Cyclotron radio emission from the giant planets of the Solar system occurs at a frequency close to the gyrofrequency, proportional to the maximum magnetic field (Zarka 1998).

Indirect methods are used to estimate the magnetic field of exoplanets (Shkolnik et al. 2005, Kislyakova et al. 2014, Ben-Jaffel et al. 2021) which rely on different assumptions. For example, Kislyakova et al. (2014), based on observations of the transit of the exoplanet HD 209458 b in the line Ly-α of the host star found strong absorption in its blue and red wings, which they interpreted as the escape of accelerated hydrogen atoms from the exosphere. The authors concluded that acceleration is possible under the influence of stellar radiation pressure, due to charge exchange with stellar wind particles, as well as due to the natural broadening of spectral lines. Based on observations, there is an extensive hydrogen corona around the planet. To explain these observations, Kislyakova et al. (2014) suggested the existence of a magnetic field of the exoplanet HD 209458 b with a magnetic moment of $\sim 1.6\times10^{26}$ A$\times$m^2, obtained from the condition of pressure balance at the daytime magnetopause. It was supposed that the pressure of the magnetosphere is magnetic, and the pressure of the stellar wind is dynamic.

In this paper, we clarify the magnitude of the magnetic field of the exoplanet HD 209458 b using observational data on its transit and available published data on the stellar wind at its orbit. These data made it possible to clarify all components of the stellar wind pressure and recalculate the planet's magnetic moment from the pressure balance at the frontal magnetopause. As noted in Zhilkin and Bisikalo (2019), for hot Jupiters in the sub-Alfvénic, the magnetic pressure of the stellar wind can exceed the dynamic pressure.

The exoplanet HD 209458 b is on a very close orbit to its host star. It is located near the Alfvén radius, at which the Alfvén Mach number M_A is equal to 1. When a planet is in a region where $M_\mathrm{A} > 1$, a comet-like magnetosphere appears around it with a bow shock in front of it, as occurs with the planets in the Solar system. If the parameters of the stellar wind are such that $M_\mathrm{A} < 1$, Alfvén wings are formed, replacing the magnetosphere, and the bow shock disappears. To calculate the magnetic field in the vicinity of the exoplanet HD 209458 b, we used a paraboloid model of the magnetosphere developed at the Institute of Nuclear Physics, Moscow State University, for planets of the Solar system and exoplanets (Alexeev 2010, Belenkaya 2024, Belenkaya et al. 2022, 2024). It will be shown how, with changing conditions in the stellar wind, a gradual transition occurs between two flow regimes with a restructuring of the magnetospheric current systems.

2 Star HD 209458

HD 209458 is a yellow dwarf of spectral class G0V (del Burgo & Allende Prieto 2016) in the constellation Pegasus, which is located at a distance of 157.5 light years from Earth (or 48.3 pc). This star is comparable to the Sun in its characteristics: mass – 1.07 $M_\odot = 2.12\times10^{30}$ kg, where $M_\odot = 1.98\times10^{30}$ kg is the mass of the Sun (Rosenthal et al. 2021); radius – 1.2 $R_\odot = 8.346\times10^5$ km, where $R_\odot = 6.955\times10^5$ km is the

radius of the Sun (Rosenthal et al. 2021); temperature – 6026 K (Rosenthal et al. 2021); age – 3.1 billion years (Bonomo et al. 2017). The magnetic moment (assumed to be equal to the magnetic moment of the Sun) is 3×10^{27} G$\times$m^3 or 3.5×10^{29} A$\times$m^2 (Humphreys 2008).

3 Exoplanet HD 209458 b

Exoplanet HD 209458 b, also known as Osiris (since 2023, the International Astronomical Union has canceled this name as the official one of the planet) is a gas giant discovered in 1999 using the transit and radial velocity methods. HD 209458 b is very close to its host star, at a distance of $R_{\rm orb}$ = 0.047 AU = 7.1×10^6 km on an orbit with zero eccentricity; its orbital period τ is ∼3.5 Earth's days. The planet is always turned to the star with one side (Stassun et al. 2017). It has the following characteristics[2]: mass – 0.73 $M_{\rm Jup}$ = 1.39×10^{27} kg, where $M_{\rm Jup}$ = 1.9×10^{27} kg is a mass of Jupiter[3]; radius $R_{\rm pl}$ = 1.39 $R_{\rm Jup}$ = 97.17×10^3 km, where $R_{\rm Jup}$ = 69.91×10^3 km is a radius of Jupiter; density is 333 kg/m^3 (Bonomo et al. 2017); equilibrium temperature[4] equals 1316 K (for details of the temperature distribution in the HD 209458 b atmosphere, see Bisikalo et al. (2013)).

4 Stellar wind flowing around HD 209458 b

Kislyakova et al. (2014), analyzing the interaction of HD 209458 b with the stellar wind, noted that transit observations are well described under the assumption of the existence of an exoplanet magnetic field that stops the wind at a distance $R_{\rm mp}$ = 2.9 $R_{\rm pl}$. In this case, the width of the obstacle is about $3R_{\rm pl}$. The exosphere interacts directly with the stellar wind. Neutral hydrogen atoms experience both charge exchange and ionization by energetic electrons from the stellar wind. As a result, the number of accelerated neutral hydrogen atoms increases, which leads to excess absorption during transit.

Studying the interaction of an exoplanet with the stellar wind, one must take into account its orbital velocity. Due to the small eccentricity, the orbit can be considered circular, and the orbital speed of the planet is equal to:

$$V_{\rm pl} = \frac{2\pi R_{\rm orb}}{\tau} = \frac{2\pi \times 7.1 \times 10^6\,{\rm km}}{302400\,{\rm s}} = 147.4\,\frac{\rm km}{\rm s} \qquad (1)$$

The total velocity of the stellar wind $V_{\rm m}$ relative to the exoplanet, taking into account the orbital $V_{\rm pl}$, is (see Fig. 1):

[2]NASA Exoplanet Archive: HD 209458 b (https://science.nasa.gov/exoplanet-catalog/hd-209458-b/)

[3]NASA: Jupiter (https://science.nasa.gov/jupiter/jupiter-facts/)

[4]Open Exoplanet Catalogue: HD 209458 b (https://www.openexoplanetcatalogue.com/planet/HD209458b/)

$$|\overrightarrow{V_{\rm m}}|^2 = |\overrightarrow{V_{\rm sw}}|^2 + |\overrightarrow{V_{\rm pl}}|^2; V_{\rm m} = \sqrt{V_{\rm sw}^2 + V_{\rm pl}^2} = \sqrt{\left(400\,\frac{\rm km}{\rm s}\right)^2 + \left(147.4\frac{\rm km}{\rm s}\right)^2} \approx 426\frac{\rm km}{\rm s} \quad (2)$$

The speed of the stellar wind $V_{\rm sw}$ is the same as for the solar wind, since the star HD 209458 is a type of the Sun. All other parameters of the stellar wind were also considered to be the same as those of the solar wind.

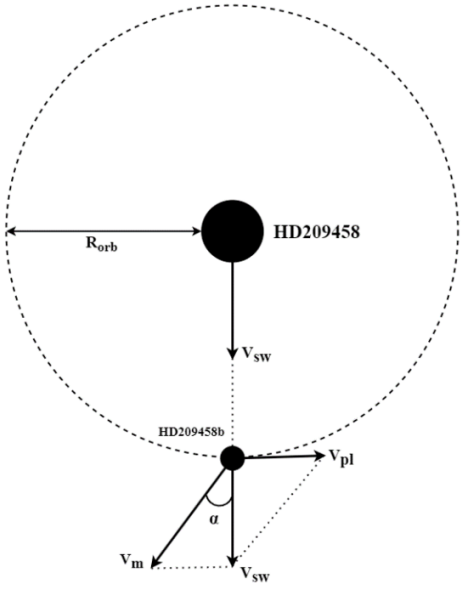


Figure 1 Scheme for calculating $V_{\rm m}$ for HD 209458 b (view from above).

The angle by which the orbital velocity will rotate the X-axis of the magnetosphere of HD 209458 b: $\alpha = \arccos(V_{\rm sw}/V_{\rm m}) \approx 20^\circ$.

To clarify the magnetic field of the exoplanet, we took into account the thermal and magnetic pressure of the stellar wind together with the dynamic pressure. Then from the equality of the total pressure of the stellar wind at the substellar point of the magnetopause and the magnetic pressure of the magnetospheric field, we obtain an expression for the distance to the frontal point $R_{\rm mp}$ (Nichols & Milan 2016):

$$R_{\rm mp} = R_{\rm pl}\left(\frac{k_{\rm m}^2 B_{\rm p}^2}{2\mu_0(k_{\rm sw}p_{\rm dyn\,sw} + p_{\rm mag\,sw} + p_{\rm th\,sw}}\right)^{\frac{1}{6}} \quad (3)$$

Here $k_{\rm m} = 2.44$ is a coefficient describing the enhancement of the magnetospheric magnetic field at the nose magnetopause by magnetopause currents (Mead & Beard 1964, Alexeev 2005); $k_{\rm sw} = 0.88$ is a coefficient for monatomic stellar wind flux (Spreiter & Alksne 1969); $p_{\rm dyn\,sw} = n_{\rm sw} m V_{\rm m}^2$ is a dynamic pressure of the stellar wind; $n_{\rm sw} = 5{\times}10^9$ m^{-3} (Kislyakova et al. 2014) is the density of stellar wind particles; $m = 1.92{\times}10^{-27}$ kg (Nichols & Milan 2016) is the average mass of particles in the stellar

wind; $p_{\text{th sw}} = n_{\text{sw}} k T_{\text{sw}}$ is thermal pressure of the stellar wind with temperature T_{sw}; $p_{\text{mag sw}} = \dfrac{B_{\text{sw}}^2}{2\mu_0}$ is magnetic pressure of the stellar wind; B_{sw} is the magnetic field of the stellar wind.

Magnetic field magnitude of the stellar wind at a distance $R_{\text{orb}} = 7.1{\times}10^9$ m: $|B_{\text{sw}}| = \sqrt{B_{\text{r}}^2 + B_{\varphi}^2 + B_{\theta}^2}$. $B_{\text{r}} = B_0 \Big(\dfrac{R_{\text{s}}}{R_{\text{orb}}}\Big)^2$ is the radial component of the magnetic field (Nichols & Milan 2016); $B_{\varphi} = B_{\text{r}} \dfrac{\Omega_{\text{s}} R_{\text{orb}}}{V_{\text{sw}}}$ is the azimuthal component of the magnetic field (Nichols & Milan 2016); $B_{\theta} = \dfrac{M \sin(\theta)}{R_{\text{orb}}^3}$ is the vertical component of the magnetic field (dipole approximation). B_0 is the magnetic field at the solar surface equal to 143000 nT = 1.43 G (Nichols & Milan 2016). Ω_{s} is the angular velocity of the Sun equal to $2.9{\times}10^{-6}$ rad/s (Nichols & Milan 2016). Thus, the values of the magnetic field and stellar wind pressure components are equal:

$$B_{\text{r}} = 143000\,\text{nT} \times \left(\frac{8.346 \times 10^8\,\text{m}}{7.1 \times 10^9\,m}\right)^2 \approx 1373\,\text{nT};$$

$$B_{\varphi} = 1373\,\text{nT} \times \frac{2.906 \times 10^{-6}\,\dfrac{\text{rad}}{\text{s}} \times 7.1 \times 10^9\,\text{m}}{400 \times 10^3\,\dfrac{\text{m}}{\text{s}}} \approx 70.8\,\text{nT};$$

$$B_{\theta} = \frac{143000 \times 10^{-9}\,\text{T} \times (8.436 \times 10^8\,\text{m})^3 \times \sin(90^\circ)}{(7.1 \times 10^9\,\text{m})^3} \approx 232\,\text{nT};$$

$$|B_{\text{sw}}| = \sqrt{(1373\,\text{nT})^2 + (70.8\,\text{nT})^2 + (232\,\text{nT})^2} \approx 1393.5\,\text{nT};$$

$$p_{\text{dyn sw}} = 9.6 \times 10^{-18}\,\frac{\text{kg}}{\text{m}^3} \times \left(426 \times 10^3\,\frac{\text{m}}{\text{s}}\right)^2 \approx 1.742 \times 10^{-6}\,\text{Pa} = 1742\,\text{nPa};$$

$$p_{\text{th sw}} = 5 \times 10^9\,\text{m}^{-3} \times 1.38 \times 10^{-23}\,\frac{\text{J}}{\text{K}} \times 1.1 \times 10^6\,\text{K} \approx 7.6 \times 10^{-8}\,\text{Pa} = 76\,\text{nPa};$$

$$p_{\text{mag sw}} = \frac{(1393.5 \times 10^{-9}\,\text{T})^2}{2 \times 4\pi \times 10^{-7}\,\dfrac{\text{H}}{\text{m}}} \approx 7.726 \times 10^{-7}\,\text{Pa} = 773\,\text{nPa}$$

Based on the obtained values, we can calculate the magnetic field of HD 209458 b at the equator:

$$B_p = \sqrt{\frac{2\mu_0 (k_{\text{sw}} p_{\text{dyn sw}} + p_{\text{mag sw}} + p_{\text{th sw}}) \times (2.9)^6}{k_{\text{m}}^2}} \approx 24456\,\text{nT} \tag{4}$$

Then the magnetic moment of the exoplanet is:

$$B_{\text{p}} \times R_{\text{pl}}^3 = 24456 \times 10^{-9}\,\text{T} \times (9.54 \times 10^7\,\text{m})^3 = 2.123 \times 10^{19}\,\text{T} \times \text{m}^3$$

Since we took into account not only the dynamic, but also the thermal and magnetic pressure of the stellar wind, the resulting magnetic field of the exoplanet at its equator B_{p} and its magnetic moment are refined. These refined parameters will be further used in the paraboloid model in calculations.

5 Paraboloid model of the magnetosphere

In this work, we will use a paraboloid model developed in the laboratory of planetary magnetospheres of the Institute of Nuclear Physics of Moscow State University for the magnetospheres of planets of the Solar system and some exoplanets (Alexeev 2010, Belenkaya et al. 2022, 2024). To describe the magnetospheric field of an exoplanet, in the paraboloid model of the magnetosphere, two current systems are added to the field of the planetary dipole: currents at the magnetopause and tail currents (if there is no magnetodisk in the magnetosphere). Currents at the magnetopause screen the magnetospheric field. The tail current system forms two lobes of field lines, separated by the tail current sheet. The interplanetary magnetic field (IMF) can partially penetrate the magnetosphere.

The described model of the magnetosphere received the name "paraboloid" because of the shape of the surface – a paraboloid of revolution, which approximates the boundary of the magnetosphere – the magnetopause:

$$\frac{x}{R_{\rm mp}} = 1 - \frac{y^2 + z^2}{2R_{\rm mp}^2} \tag{5}$$

Here the X axis is oriented from the center of the planet in the direction to the star, the Y axis is directed towards the evening, and the Z axis is directed towards the north of the planet, perpendicular to the X and Y axes. This coordinate system is called stellar-magnetospheric. The parameter $R_{\rm mp}$ is the distance from the center of the planet to the substellar point of the magnetopause. It is the main parameter of the magnetosphere, characterizing its scale. According to observations (Kislyakova et al. 2014), it is equal to:

$$R_{\rm mp} = 2.9R_{\rm pl}$$

The remaining parameters of the magnetosphere model for the case under consideration are described in Belenkaya (2024). Distance to the inner edge of the tail current sheet $R_2 \sim 0.7R_{\rm mp}$; magnetic field of the tail current system at a distance R_2: $B_{\rm t} = -1.2B_{\rm p}(R_{\rm pl}/R_{\rm mp})^3$.

6 Passing through the Alfvén radius

At the Alfvén radius, the Alfvén Mach number $M_{\rm A}$ is 1. Before it, the stellar wind is sub-Alfvénic, and beyond it it is super-Alfvénic. Alfvén Mach number: $M_{\rm A} = \dfrac{V_{\rm m}}{V_{\rm A}}$; $V_{\rm A} = \dfrac{B_{\rm sw}}{\sqrt{\mu_0 \rho_{\rm sw}}}$ is the Alfvén speed; $\rho_{\rm sw} = n_{\rm sw}{\rm m}$ is the stellar wind density:

$$\rho_{\rm sw} = 5 \times 10^9\,{\rm m}^{-3} \times 1.92 \times 10^{-27}\,{\rm kg} \approx 9.610^{-18}\,{\rm kg} \times {\rm m}^{-3};$$

$$V_{\rm A} = \frac{1393.5\,{\rm nT}}{\sqrt{4\pi \times 10^{-7}\,\dfrac{\rm H}{\rm m} \times 9.6 \times 10^{-18}\,{\rm kg} \times {\rm m}^{-3}}} \approx 401\,\frac{\rm km}{\rm s};$$

$$M_{\rm A} = \frac{426\,\dfrac{\rm km}{\rm s}}{401\,\dfrac{\rm km}{\rm s}} \approx 1.06 \approx 1$$

The closeness of the obtained value $M_{\rm A}$ to unity indicates that this is a borderline case, i.e. from time to time, depending on stellar activity, the Alfvén Mach number can be either greater or less than unity. In the case when $M_{\rm A}$ is less than unity, not a comet-like magnetosphere with a bow shock in front of it should be formed, but Alfvén wings without a bow shock. In those moments when $M_{\rm A}$ becomes greater than unity, a comet-like magnetosphere with a bow shock ahead of it, usual for the Solar system, will appear. Both cases will be discussed in more detail below. During the modeling process, we will assume that the magnetic dipole of HD 209458 b is oriented to the south, like that of the Earth.

7 Magnetosphere of HD 209458 b depending on the IMF components at $M_{\rm A} > 1$

To begin our study of the interaction between the magnetosphere of an exoplanet and the stellar wind, let us consider the case of zero interplanetary magnetic field (IMF) (Fig. 2).

In this case, we have a closed magnetosphere, the open magnetic field lines of which go into the distant tail without crossing the magnetopause.

Let us consider how the magnetosphere changes under the influence of a nonzero IMF. The paraboloid model takes into account the interplanetary magnetic field, which partially penetrates the magnetosphere. The penetration coefficient k is taken to be about 0.2, like that of the Earth. First, let us consider the most significant

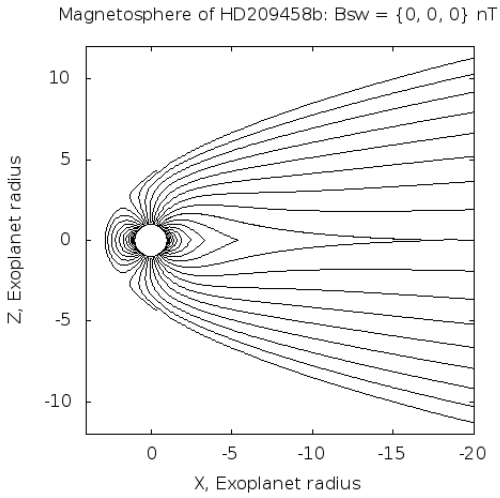


Figure 2 Magnetosphere of exoplanet HD 209458 b at zero IMF.

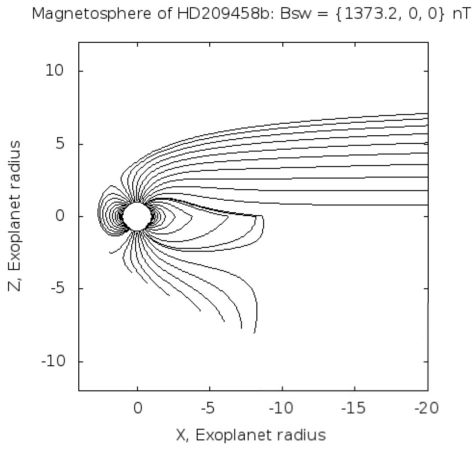


Figure 3 Magnetosphere of exoplanet HD 209458 b in the presence of a positive radial component of stellar wind's magnetic field for southward planetary magnetic moment.

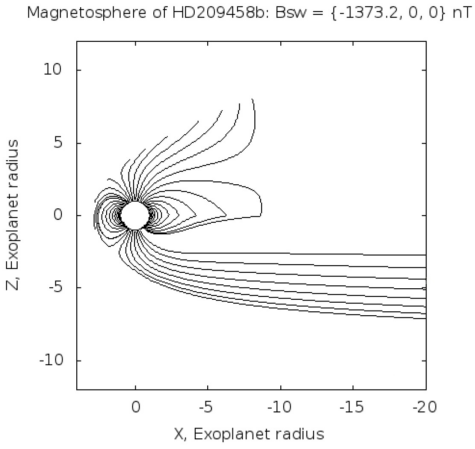


Figure 4 Magnetosphere of HD 209458 b in the presence of a negative radial component of stellar wind's magnetic field for southward planetary magnetic moment.

component of the IMF in a close orbit of an exoplanet – it is the radial one. The radial component sharply changes the magnetospheric field (Fig. 3).

Figure 3 shows the open field lines of the two polar caps. In the northern hemisphere, the field lines of the northern polar cap gather in a tail along the planet-star line. In the southern hemisphere, the open field lines of the lower lobe of the tail, associated with the southern polar cap, turn and cross the southern magnetopause. There is a sharp separation between the lines emerging from the southern polar cap and the lines entering the northern one. This structure arises due to field enhancement in the northern lobe of the magnetotail and weakening in the southern lobe as a result of the strong influence of the positive radial component of the IMF, which partially penetrates the magnetosphere.

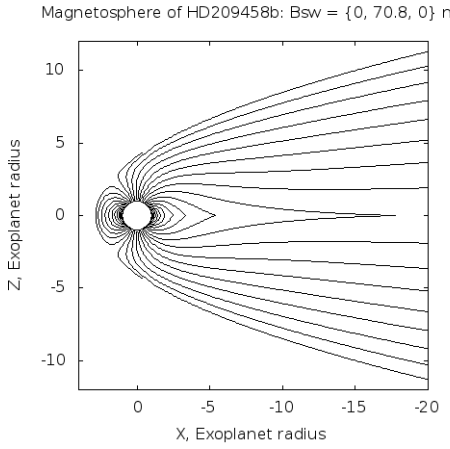


Figure 5 Magnetosphere of HD 209458 b in the presence of a small azimuthal component of stellar wind's magnetic field.

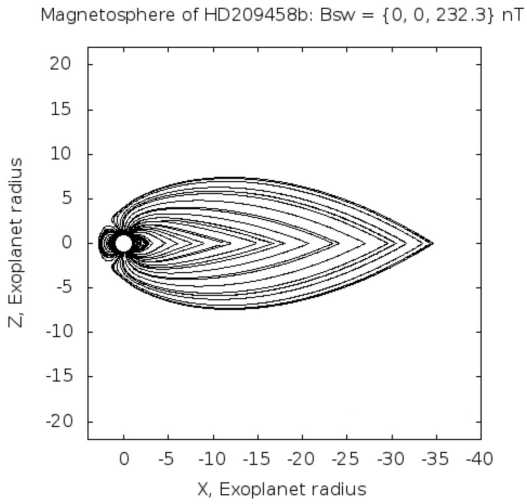


Figure 6 Magnetosphere of HD 209458 b in the presence of a positive vertical component of stellar wind's magnetic field.

When the radial component changes sign (Fig. 4), we get a picture symmetrical to Fig. 3 relative to the planet-star line: the negative radial component of the IMF strengthens the extended tail in the southern hemisphere and weakens it in the northern hemisphere. The shortened tail is now in the northern part of the magnetosphere.

The second component of the IMF is azimuthal. Because its value is relatively small, it does not have a serious effect on the structure of the magnetosphere; the resulting picture (Fig. 5) is almost no different from the case of zero IMF (Fig. 2).

The third component is vertical. For a northward IMF, the magnetosphere of an exoplanet with a southward magnetic dipole axis becomes closed (Fig. 6).

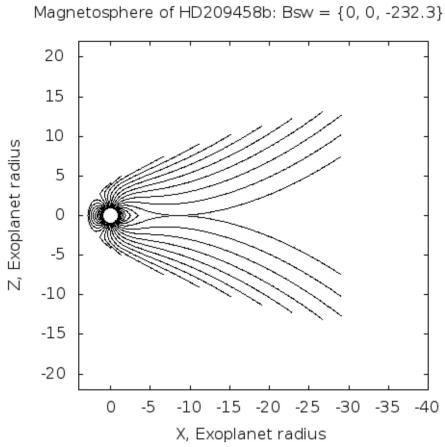


Figure 7 Magnetosphere of HD 209458 b in the presence of a negative vertical component of stellar wind's magnetic field.

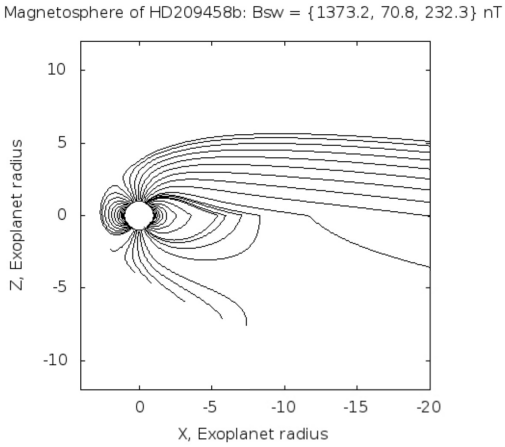


Figure 8 Magnetosphere of HD 209458 b with all components of stellar wind's magnetic field.

When the sign of the vertical component changes (i.e., the southward IMF), the magnetosphere becomes open (Fig. 7), similar to the Earth's magnetosphere with the southward IMF.

As a result of modeling the magnetosphere with all three IMF components, we obtained Fig. 8, which is very similar to Fig. 3. The most significant contribution is made by the radial component – it is larger than the others and radically changes the field structure of the magnetosphere. However, the contribution of the vertical component is also noticeable – the lines of the northern hemisphere slightly change their direction, crossing the planet-star line.

8 Magnetosphere of HD 209458 b depending on the IMF components at $M_A < 1$

As mentioned earlier, we have a borderline case (the Alfvén Mach number is close to unity), therefore, when the parameters of the stellar wind change so that $M_A < 1$, the magnetosphere of HD 209458 b can take the form of Alfvén wings. The Alfvén Mach number depends on three quantities – the total velocity of the stellar wind V_m, the mass density of the stellar wind ρ_{sw} and the magnetic field of the stellar wind B_{sw}. Within the paraboloid model, we can only change the magnitude of the magnetic field of the stellar wind, so all subsequent simulations will be carried out with an increase in the parameter B_{sw} and its individual components (radial, azimuthal and vertical), which can be explained, for example, by stellar activity (the flare on HD 209458). Ridley (2007) have used a similar method; he obtained Alfvén wings in the MHD model for the Earth, enhancing the IMF by 12 times. In the new version of the paraboloid model for Alfvén wings, the condition for stopping counting at the magnetopause is removed.

Just as in the case of a cometary magnetosphere, let us first consider the most significant component of the IMF in a close orbit – the radial one. Figures 9 and 10 show structures of the magnetosphere corresponding to an IMF amplification of 5 and 10 times, respectively. The field lines are strongly compressed on the day side due to the pressure of the stellar wind, but on the night side they stretch out and form a long tail (in the northern hemisphere for positive radial IMF and southward magnetic planetary dipole) lying along the planet-star line.

Figure 9 shows how in the southern hemi-space two bundles of open field lines are formed separated by a cusp. One was obtained from a rotated beam of open tail field lines, the second from closed field lines of the dayside magnetosphere, which became

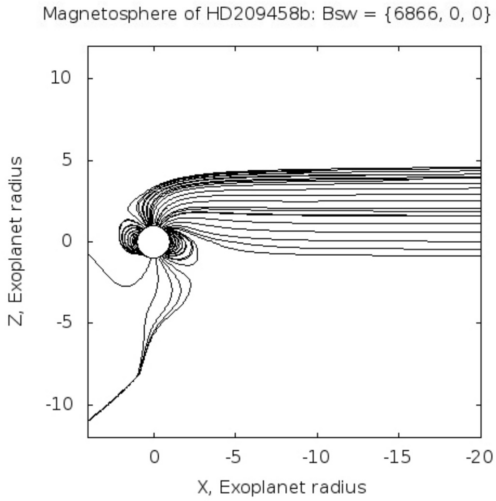


Figure 9 Magnetosphere of HD 209458 b with a 5-fold increase in the radial component of stellar wind's magnetic field.

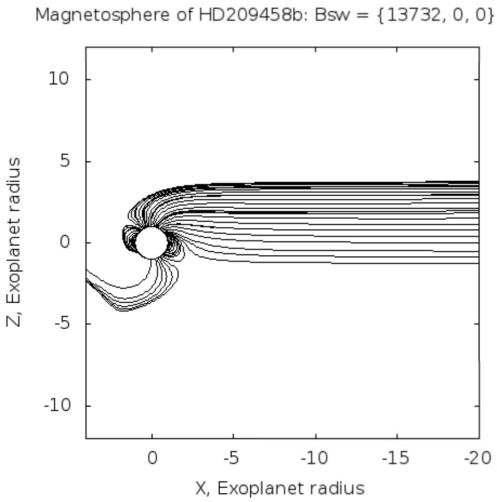


Figure 10 Magnetosphere of HD 209458 b with a 10-fold increase in the radial component of stellar wind's magnetic field.

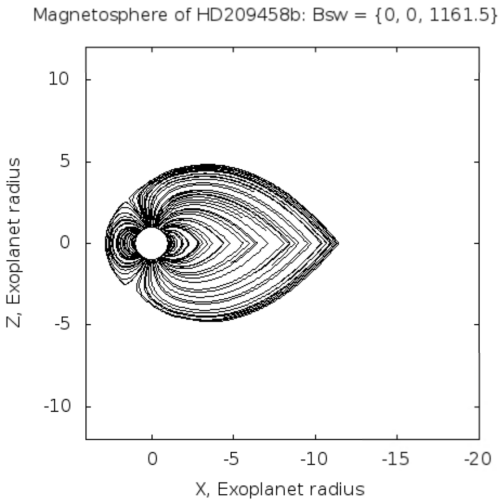


Figure 11 Magnetosphere of HD 209458 b with a 5-fold increase in the vertical component of stellar wind's magnetic field.

open due to an increase in the radial magnetic field. The azimuthal component, due to its smallness relative to other components, does not significantly change the structure of the magnetosphere. When the IMF is amplified by 5 and 10 times, we have a qualitatively similar picture as before (Fig. 2, Fig. 5) – a closed magnetosphere, the open field lines of which form a tail. The last component is vertical. For a northward IMF, the magnetosphere of an exoplanet with a dipole axis directed to the south

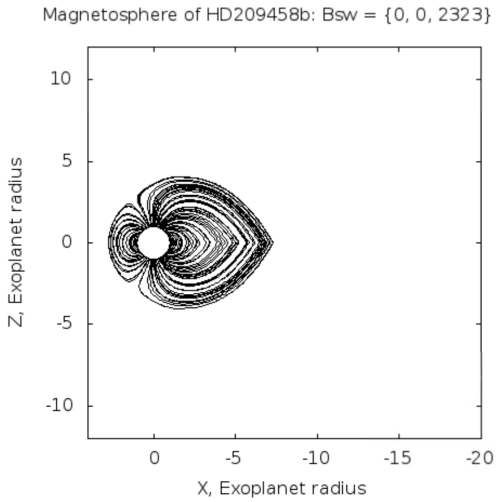


Figure 12 Magnetosphere of HD 209458 b with a 10-fold increase in the vertical component of stellar wind's magnetic field.

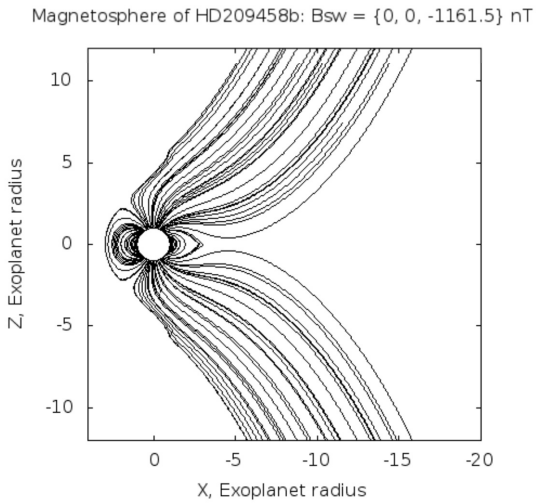


Figure 13 Magnetosphere of HD 209458 b with a 5-fold increase in the negative vertical component of stellar wind's magnetic field.

becomes closed; as the IMF strengthens, the magnetosphere is compressed in all directions (Figs 11 and 12).

When the sign of the vertical component changes (i.e. the IMF is directed to the southward), the magnetosphere becomes open (Figs 13 and 14), and pronounced Alfvén wings are formed, in which the angle of deviation from the planet-star line increases as the IMF strengthens.

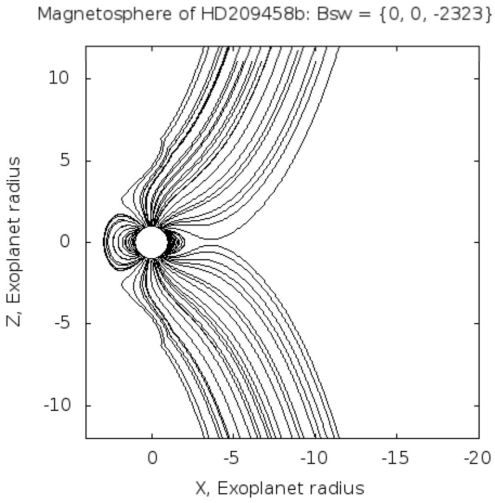


Figure 14 Magnetosphere of HD 209458 b with a 10-fold increase in the negative vertical component of stellar wind's magnetic field.

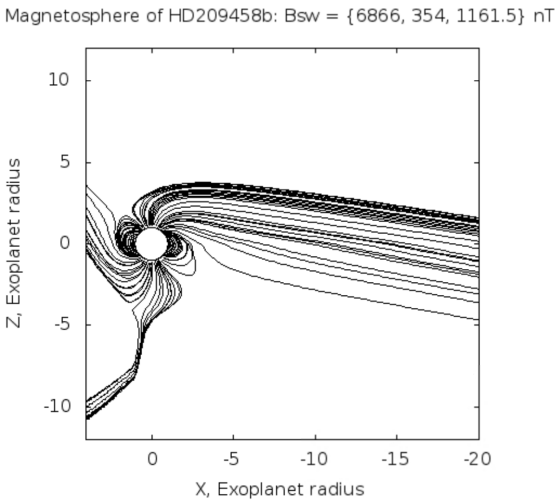


Figure 15 Magnetosphere of HD 209458 b with all stellar wind's magnetic field components amplified by a factor of 5.

As a result of modeling the magnetosphere taking into account all three enhanced IMF components, we obtained Figs 15 and 16.

The most significant contribution, as in the case of a comet-like magnetosphere, is made by the largest radial component – it radically changes the field of the magnetosphere: Alfvén wings, formed by the field lines of the northern and southern hemispheres, extend along the planet-star line, but have opposite directions. As in the case of a comet-like magnetosphere, the contribution of the vertical component is

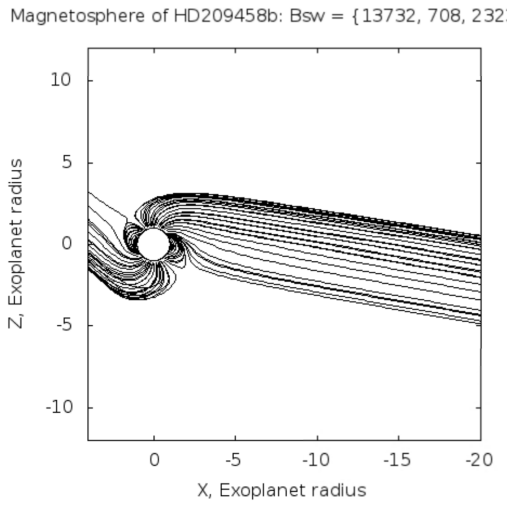


Figure 16 Magnetosphere of HD 209458 b with all stellar wind's magnetic field components amplified by a factor of 10.

noticeable – the lines of the northern and southern hemispheres change their direction, crossing the planet-star line.

Figure 15 again shows the division in the southern half-space of night and day open field lines (separated by the cusp). The result obtained for the total IMF at $M_A < 1$ and presented in Fig. 16 is in good agreement with the results of MHD simulations around HD 209458 b for this case (Zhilkin & Bisikalo 2019, 2020; Zhilkin et al. 2020).

In this work, in contrast to Belenkaya (2024), we consider the influence of not only the vertical component of the IMF, but also two others; the radial component plays the main role due to the close location of the planet to the solar-type star.

9 Conclusions

Using the available published data on the star HD 209458 system, a paraboloid model of the exoplanet's HD 209458 b magnetosphere was constructed. In the process of work, the parameters of the paraboloid model were determined, the magnetic field at the equator of the planet was refined by including the magnetic and thermal pressures of the stellar wind, and various structures of the magnetic field of the magnetosphere were obtained depending on the magnitude and direction of the IMF. In the case when the Alfvén Mach number is greater than unity, a comet-like structure of the magnetosphere with a bow shock ahead of it, typical of the planets of the Solar system, was obtained. A change in the sign of the radial and azimuthal IMF components leads to symmetrical changes in the structure of the magnetosphere relative to the XY and XZ planes, respectively. A change in the sign of the vertical component of the IMF leads to a significant change – a transition from a closed magnetosphere to an open one. In the case when the Alfvén Mach number is less than unity (this condition is met due

to the strengthening of the magnetic field of the stellar wind), a magnetosphere with Alfvén wings was obtained. The Alfvén wings are most clearly visible in the case of a negative vertical IMF component for the southward magnetic field of the exoplanet. When all three components are taken into account, two Alfvén wings are extended along the planet-star line in different directions (due to the influence of the vertical component, the flows are slightly rotated relative to the X axis). The work shows that the transition from the super-Alfvénic to the sub-Alfvénic flow regime occurs smoothly and not abruptly. The current systems of the tail and magnetopause in the model are not rearranged with this approach, and their contribution becomes negligibly small compared to the effect of the strong IMF, due to which this transformation is carried out. In this case, for $M_A < 1$, the currents of the tail current sheet seem to disappear, passing to the boundaries of the bundles of open field lines that form the wings. Under the influence of the radial component of the magnetic field of the stellar wind, depending on its magnitude, not 2, but 3 wings can arise. The sign of the radial component determines whether the splitting occurs in the northern or southern half-space. With a positive radial component of the IMF for the southward dipole of the planet, 2 beams of open field lines are formed in the southern half-space. One of them is obtained by turning the tail lobe bundle to the south, the other arises from daytime closed field lines under the influence of radial positive IMF. These bundles are formed on opposite sides of the cusp.

References

Alekseev I.I. (2010) VMU. Series 3. Physics. Astronomy. No 4
Alexeev (2005) American Geophysical Union, Washington, DC, p. 257
Barstow et al. (2017) The Astrophysical Journal, 834:50 (15pp)
Belenkaya E.S. (2024) Astronomy Reports, Vol. 68, No. 3, pp. 294–299
Belenkaya E.S., Alexeev I.I., Blokhina M.S. (2022) Universe, 8, No. 4
Belenkaya E.S., Alexeev I.I., Kalegaev V.V. (2024) Astronomy Reports, Vol. 68, No. 1, pp. 10-18
Ben-Jaffel, L., Ballester, G.E., Munoz, A.G. et al. (2021) Nature Astronomy, 6, 141
Bisikalo et al. (2013) Astronomy Reports, Vol.57, No.10, pp. 715-725
Bonomo et al. (2017) Astronomy & Astrophysics, 602, A107 (16pp)
del Burgo & Allende Prieto (2016) MNRAS 463, 1400-1408
Humphreys D. Russel (2008) Proceedings of the International Conference on Creationism, Vol.6, pp. 213-230
Ip & Kopp (2002) Journal of Geophysical Research, 107(A12), 1491
Jia et al. (2010) Space Science Reviews, 152(1), 271-305
Jia et al. (2008) Journal of Geophysical Research, vol. 113, A06212
Kislyakova et al. (2014) Science, 346, 981
Mead & Beard (1964) Journal of Geophysical Research, 69(7), 1169-1179
Nichols & Milan (2016) MNRAS 461, 2353-2366
Ridley (2007) Ann. Geophys., 25, 533-542
Rosenthal et al. (2021) The Astrophysical Journal Supplement Series, 255:8 (67pp)
Shkolnik, E., A.H. Walker, D.A. Bohlender, P.-G. Gu, M. Kurster (2005) The Astrophysical Journal, 622, 1075–1090

Spreiter & Alksne (1969) Reviews of Geophysics, volume 7, issue 1-2, p. 11-50
Stassun et al. (2017) The Astronomical Journal, 153:136 (20pp)
Zarka, P. (1998) Journal of Geophysical Research: Planets, 103, 20159
Zhilkin A.G., D.V. Bisikalo (2019) Astronomical Journal, volume 96, no. 7, p. 547–562
Zhilkin A.G., D.V. Bisikalo (2020) Astronomical Journal, volume 97, no. 7, p. 538–554
Zhilkin A.G., D.V. Bisikalo, P.V. Kaygorodov (2020) Astronomical Journal, volume 97, no. 2, p. 145–154